CHEMISTRY
A EUROPEAN JOURNAL

DOI: 10.1002/chem.200701428

Tautomerism in Novel Oxocorrologens

Yongshu Xie,[a, d] Jonathan P. Hill,*[a] Amy Lea Schumacher,[b] Paul A. Karr,[b] Francis D'Souza,*[b] Christopher E. Anson,[c] Annie K. Powell,[c] and Katsuhiko Ariga[a]

Abstract: A novel corrole-type macrocycle, oxocorrologen (**2**), substituted with hemiquinone groups, has been synthesized. It was found to undergo multiple tautomerism of its exchangeable protons between electronegative atom sites at the macrocyclic core (nitrogen atoms) and periphery (phenol oxygen atoms). Alkylation at one macrocyclic nitrogen atom with a 4-nitrobenzyl group gave **3**, which can exist in only two tautomeric forms depending on the solvent. Tautomerism has been studied by means of ^{1}H NMR spectroscopy in a variety of solvents and solvent mixtures. Tautomer structure assignments have been supported by DFT calculations of the relative energies of the tautomers. X-ray crystallography of the *N*-nitrobenzyl derivative has revealed that intramolecular hydrogen bonding may be responsible for stabilizing the observed tautomers. The solvent dependence of the tautomerism of **2** and **3** confers solvatochromism. Electrochemical measurements on **2** and **3** in their respective quinone forms have revealed irreversible processes, but indicate that they are both electron-deficient with a small HOMO–LUMO gap and first reduction potentials close to those of fullerene electron acceptors.

Keywords: corroles · N-alkylation · porphyrinoids · quinones · tautomerism

Introduction

Isomerism of a molecule occurring by an easy conversion between different forms as a result of the movement of one or more hydrogen atoms is known as prototropic tautomerism[1] and is intimately related to the structural identity of the respective molecule, with the isomers referred to as tautomers. Probably the most common example of the phenomenon is prototropic keto–enol tautomerism, in which an exchangeable proton can be bonded at oxygen or another electronegative atom within the same molecule yielding two distinct structures.[2] Despite its conceptual simplicity, this feature is of paramount importance in biochemical systems[3,4] and also from the point of view of chemical reactivity.[5] The existence of an individual molecule in multiple stable states is also important with regard to potential applications, especially if each state has discrete electrochemical and/or spectroscopic characteristics. This would permit the construction of molecular multi-throw switches and other devices with potential for molecular level information processing.[6,7] Tautomeric variation of molecular structure should be of use since it is a facile process that can be influenced by an external stimulus such as incident electromagnetic radiation.[8,9] In the realm of tetrapyrrole chemistry, there is no more familiar example of tautomerism than that of the porphyrin pyrrolic amine groups at the core of the macrocycle[10] or at the periphery in N-confused porphyrins.[11] Moreover, compounds containing the corrole framework are currently a subject of intensive investigation because of their exceptional properties related to advanced applications[12–14] and because of recent advances in synthetic procedures.[15] Here, we report multiple prototropic tautomerism[16] in a novel ox-

[a] Dr. Y. Xie, Dr. J. P. Hill, Dr. K. Ariga
WPI Center for Materials Nanoarchitectonics
and Supermolecules Group
National Institute for Materials Science
Namiki 1-1, Tsukuba, Ibaraki 305-0044 (Japan)
Fax: (+81) 29-860-4832
E-mail: Jonathan.Hill@nims.go.jp

[b] Dr. A. L. Schumacher, Prof. P. A. Karr, Prof. F. D'Souza
Department of Chemistry, Wichita State University
1845 Freemount, Wichita, Kansas 67260-0051 (USA)
Fax: (+1) 316-978-3431
E-mail: Francis.DSouza@wichita.edu

[c] Dr. C. E. Anson, Prof. A. K. Powell
Institute for Inorganic Chemistry
University of Karlsruhe, Geb. 30.45
Engesserstrasse 15, 76128 Karlsruhe (Germany)

[d] Dr. Y. Xie
Current address: Key Laboratory for Advanced Materials
and Institute of Fine Chemicals
East China University of Science and Technology
Meilong Rd. 130, Shanghai 200237 (PR China)

Supporting information for this article is available on the WWW under http://www.chemeurj.org/ or from the author.

ocorrologen-type molecule.[17] We also report the controlling effect on this tautomerism of alkylation at one of the central nitrogen atoms.

Results and Discussion

To address the problem of constructing a molecule possessing multiple stable states, we considered that the asymmetry of the corrole macrocycle would be of importance when combined with the tautomerism of oxoporphyrinogen **1**[18,19] (see Figure S1) and we sought to advance this idea by the design of **2**, the corrole analogue of **1**. If the molecular symmetry of **1** is broken by deliberate removal of one pyrrole–pyrrole bridging group, then compound **2** is obtained. Although oxoporphyrinogen compounds have been known for some time, the corresponding oxocorrologen compounds have not been investigated. We speculated that the quinoidal substituents might also stabilize an oxocorrologen, and this was proven by our synthesis of compound **2**. The molecule thus obtained possesses four different electronegative atom sites (as opposed to two in **1** or corrole), and as a result this molecule can exist as several possible tautomers (see Scheme 1). These tautomers can be classified according to the state of protonation at the macrocyclic nitrogen atoms. Thus, type 1 possesses four exchangeable NH protons, type 2 has three NH groups, type 3 has two NH groups, and type 4 contains one exchangeable NH proton. The synthesis of **2** was accomplished by a known method.[15]

The tautomerization of **2** can be controlled to some extent by using different solvents, as shown by the ^{1}H NMR spectra of **2** in various solvents in Figure 1. In polar solvents such as [D_6]DMSO (Figure 1a)i), b)i)), a pure tautomer is present and it can be assigned the structure **2a** since all nitrogen atoms are protonated and all oxygen atoms are nonprotonated (type 1). The spectrum features four resonances due to pyrrolic protons (in [D_6]DMSO two are overlapped) and three due to the alkene protons of the *meso*-substituents since these groups are not free to rotate. The broadness of this spectrum is most likely due to a rapid exchange of solvent hydrogen-bonded at the amino groups. Tautomer **2a** is analogous to the porphyrinogen form of compound **1**.[18] In polar media, the porphyrinogen form **2a** is present because of hydrogen bonding to the solvent molecules; indeed, oxoporphyrinogens have a known propensity to bind solvents through this interaction.[20] The resonances due to the NH protons, the *meso*-substituent alkene protons, and the pyrrolic β-protons have the expected relative integrals of 4:6:8 (see the Supporting Information). Dissolution in other solvents results in tautomeric mixtures. Tautomers **2b** (type 2) and **2c** (type 3) appear when **2** is dissolved in less polar solvents ([D_8]toluene: Figure 1a)ii), b)ii); $CDCl_3$: Figure 1a)iii), b)iii); 40% (v/v) CD_2Cl_2 in [D_{14}]hexane: Figure 1a)iv), b)iv)). Both tautomers possess phenolic protons and the type 3 structure of **2c** is assigned on the basis of the presence of two phenolic and two NH proton resonances in its ^{1}H NMR spectrum. The substantial downfield shift of the

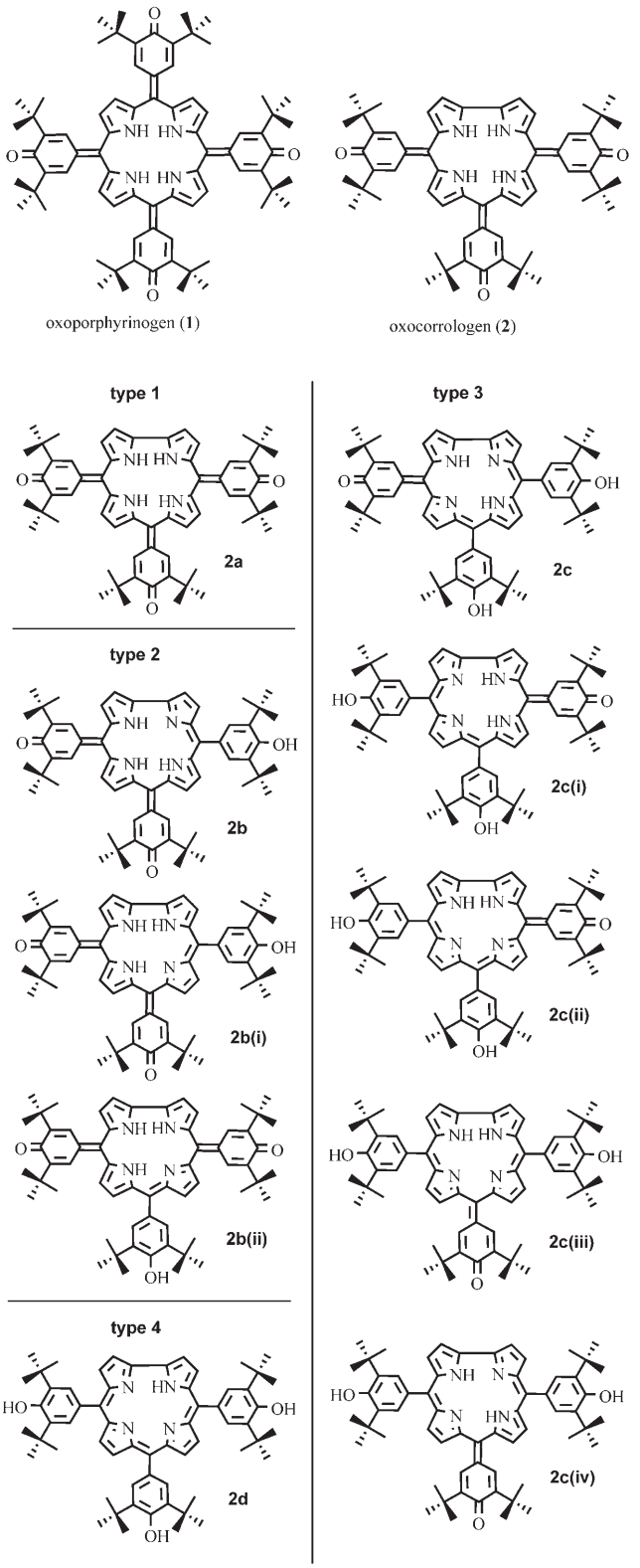

Scheme 1. Structures of compounds **1** and **2** and the possible tautomers of **2** classified according to the positions of the exchangeable protons. Note that **2d** is antiaromatic.

NH peaks indicates an intramolecular hydrogen-bonding interaction.[21] It is apparent that while a three-way tautomer-

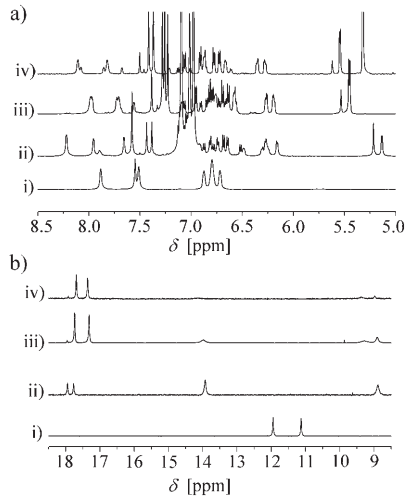

Figure 1. ^{1}H NMR spectra of **2**: a) aromatic region, b) pyrrole NH region. Solvents: i) [D_6]DMSO (**2a**), ii) [D_8]toluene (**2b**: 70%; **2c**: 30%), iii) $CDCl_3$ (**2b**: 31%; **2c**: 69%), and iv) CD_2Cl_2 in [D_{14}]hexane (40% v/v) (**2b**: 19%; **2c**: 81%).

ism is operative for compound **2**, only the tautomer **2a** is available in a demonstrably pure form at one extreme of solvent polarity. **2b** is not isolable, being present at a maximum level of $\approx$70% in [D_8]toluene, and the maximum level of **2c** is about 80% at the other accessible extreme of solvent non-polarity in this system. Interestingly, the tautomerism of **2** does not extend detectably to an isomer containing three phenolic protons (i.e., a type 4 tautomer) under any conditions. This is most probably due to the antiaromatic character and hence the reduced stability of type 4 tautomers.[22] Alternatively, the polarity-dependent trend towards stability of the more highly phenol-substituted tautomers suggests that a medium of extremely low polarity might be necessary to observe this species, although decreasing solubility in nonpolar solvents such as hexane may preclude such an observation.

Since the tautomerism of **2** is sensitive to solvent polarity, we used this fact, in conjunction with correlation NMR and NOE NMR spectroscopies, to determine the identities of the tautomers present among the possible tautomeric structures. Initially, the NH/OH ratio of the tautomers could be deduced from the 1D proton NMR spectra since *meso*-substituents such as phenol groups should be rotatable and this is reflected in the presence of a singlet resonance due to the phenyl protons of these substituents. The relative peak areas of the resonances in spectra of mixtures of tautomers can be used to assign resonances to particular tautomers. Overlapping peaks can also be detected from the integrated intensities. Peaks due to phenol resonances are also a good indicator of the tautomer type since types 1, 2, and 3 contain no, one, and two exchangeable phenol protons, respectively. In the present case, it is fortuitous that a) tautomer **2a** is available in pure or nearly pure form, b) resonances in the spectra of mixtures of tautomers **2b** and **2c** in [D_8]toluene are very well resolved, c) resonances in the spectra of mixtures of tautomers **2b** and **2c** in CD_2Cl_2/[D_{14}]hexane or $CDCl_3$ are also reasonably well resolved, d) when the pyrrole N is protonated, that is, NH, resonances due to protons attached to the pyrrole β-positions are broader than those of protons on pyrrole groups with imine-type nitrogen atoms. First, 2D-COSY spectra were used to determine resonances due to pyrrole protons attached to the same pyrrole nucleus, and to determine which *meso*-substituent resonances were related. Subsequently, a combination of qualitative steady-state NOE experiments and 2D-NOESY spectra was used to collect information on the relative positions of the pyrrole units and the *meso*-substituents. As a starting point for the assignments, we located the resonances due to the aromatic protons of the phenolic substituents since these appear as simple singlets and should stimulate NOE responses with two pyrrole groups. Irradiation of the protons of the alkene or aromatic units of the *meso*-substituents, in conjunction with the 2D-COSY spectra, proved sufficient to assign the relative positions of the pyrrole groups and *meso*-substituents. Either correlations due to long-distance coupling between the pyrrole NH and the corresponding β-H or line broadening in the 1D proton NMR spectra revealed the positions of the NH groups. Protons adjacent to the corrole pyrrole–pyrrole bond were assigned on the basis of their lack of NOE response upon irradiation of any of the *meso*-substituent protons.

Tautomer **2a** is predominant (>95 mol%) in [D_8]THF solution, and COSY and NOESY spectra were used to assign all of its resonances (Figure 2). [D_8]THF was used as solvent because of the poor solubility of **2** in [D_6]DMSO (in which only tautomer **2a** is present). Signals between $\delta = 7.00$ and 6.75 ppm are due to the protons of the pyrrole groups, while those between $\delta = 8.00$ and 7.60 ppm are due to the protons at the *meso*-substituent (in this case, alkene-H). Correlations between these peaks in the 2D-COSY and 2D-NOESY spectra were used to confirm the structure of this tautomer and to assign the origin of the resonances. Also, resonances due to the *tert*-butyl groups could be unequivocally assigned (see the Supporting Information), and long-range couplings between pyrrole β-H and the corresponding pyrrolic amine protons were evidenced. The most upfield resonance of the pyrrole groups was assigned to the outer proton of the corrole-type pyrrole group since it showed no NOE correlation with any *meso*-substituent. Subsequent correlations are shown in Figure 2.

For tautomer **2b**, the highest molar proportion of 70% is found in [D_8]toluene. The proton NMR spectrum in [D_8]toluene could be partly assigned using 2D-COSY, but 2D-NOESY spectra were less informative because of the peaks due to residual toluene, which appeared at around $\delta = 7.0$ ppm. The structure of the oxocorrologen framework of **2b** was assigned with the aid of difference NOE spectroscopy, the relevant NOE signals being indicated in Figure 3. The resulting structure immediately discounts possible tautomer **2b(ii)**. The positions of the central protons were assigned on the basis of the broadening of the β-pyrrolic resonances of the relevant pyrrolic groups, which is caused by

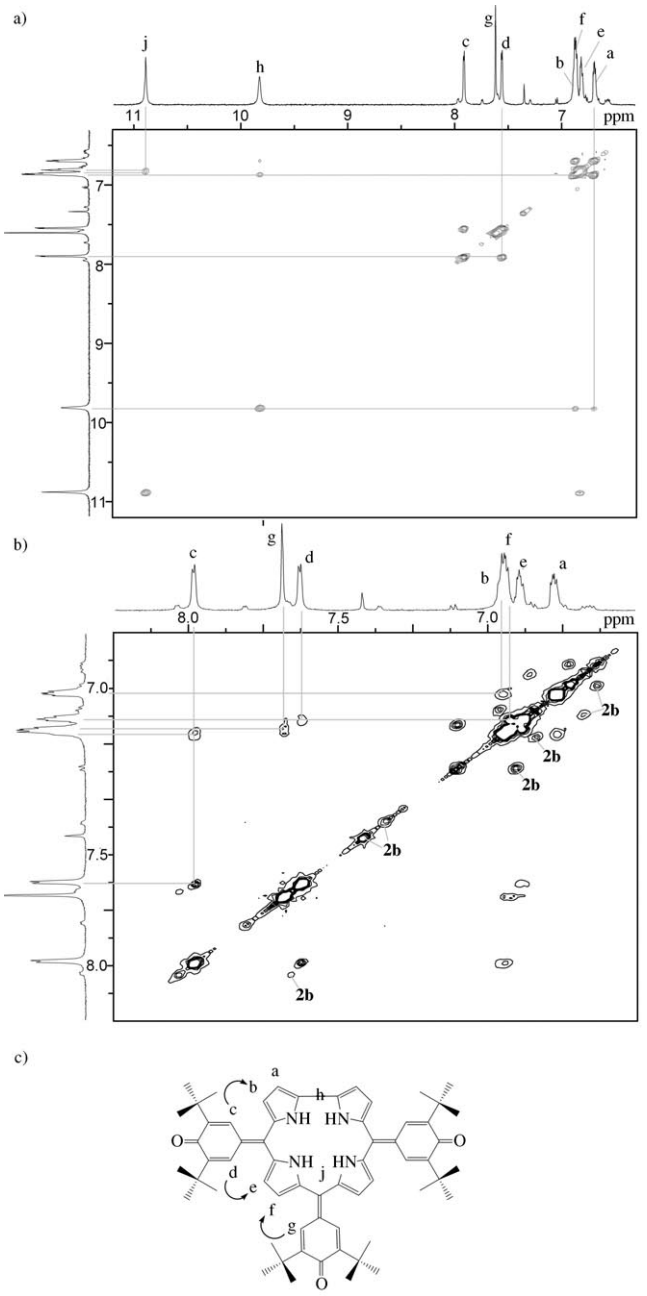

Figure 2. a) 2D-COSY (^{1}H,^{1}H) and b) 2D-NOESY (^{1}H,^{1}H) for tautomer **2a**. Minor peaks due to **2b** are labeled. c) Assignment of the resonances of **2a**, with an indication of NOE correlations (arrows).

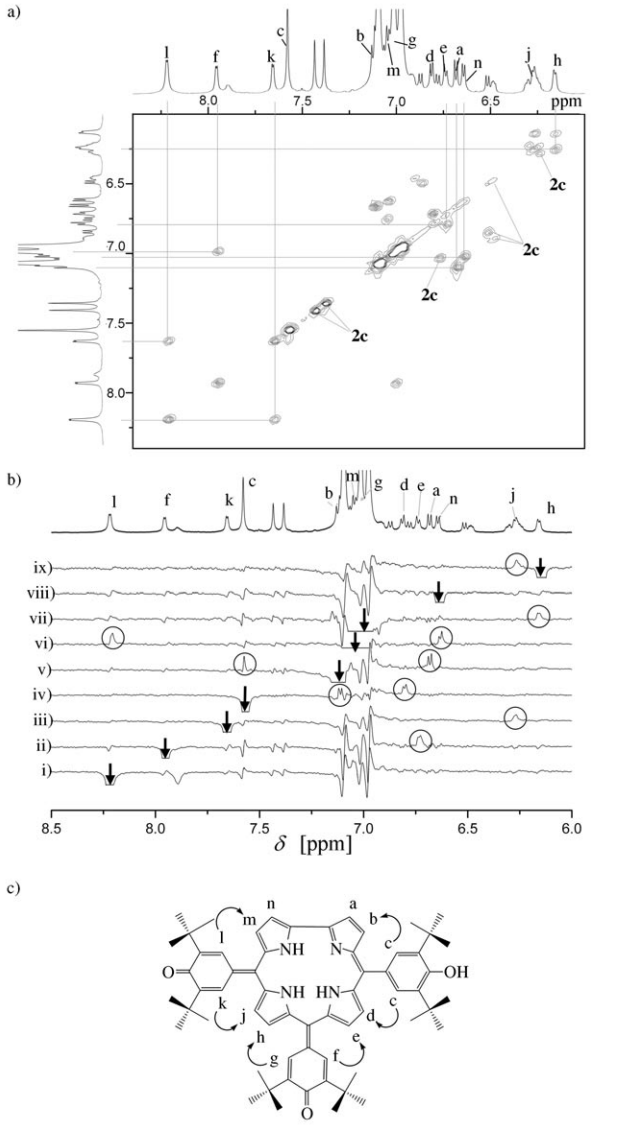

Figure 3. a) 2D-COSY (^{1}H,^{1}H) and b) i)–ix) steady-state NOE enhancements obtained by irradiation at the indicated resonances of tautomer **2b** (downward arrows). Peaks and correlations due to **2c** are indicated. The strongly negative peak at the irradiation position has been removed for clarity. c) Assignments of peaks and elicited NOEs.

long-range coupling with the respective NH protons.[23] There is one other interesting feature of the spectra of **2b**. In solutions in chlorinated solvents or tetrahydrofuran, all three amine protons are observable. However, in toluene the broadest of these peaks cannot be seen and two resonances (due to the β-H of one pyrrole group) are additionally shifted to higher field by around 0.5 ppm.

For tautomer **2c** in $CDCl_3$ (Figure 4), NOE correlations between two *meso*-phenol substituents and resonances from a single pyrrole group already discount tautomers **2c(iii)** and **2c(iv)**. While the phenol substituents both give the two NOE signals expected from their free rotation, irradiation of either of the alkene protons on the quinone group unexpectedly results in an NOE enhancement for two pyrrolic protons as well as a negative peak for the remaining alkene proton on the same substituent. Additionally, resonances due to quinone alkene protons are usually broad and sharpen at decreased temperatures, suggesting some dynamic process. To explain these phenomena, we consulted a molecular model of **2c**. In the model (Figure 5), the phenol groups show the expected non-coplanarity with the oxocorrole macrocycle, but the quinone group also displays a marked and unexpected non-coplanarity. Furthermore, there appear to be two possible extremes of this arrangement, although

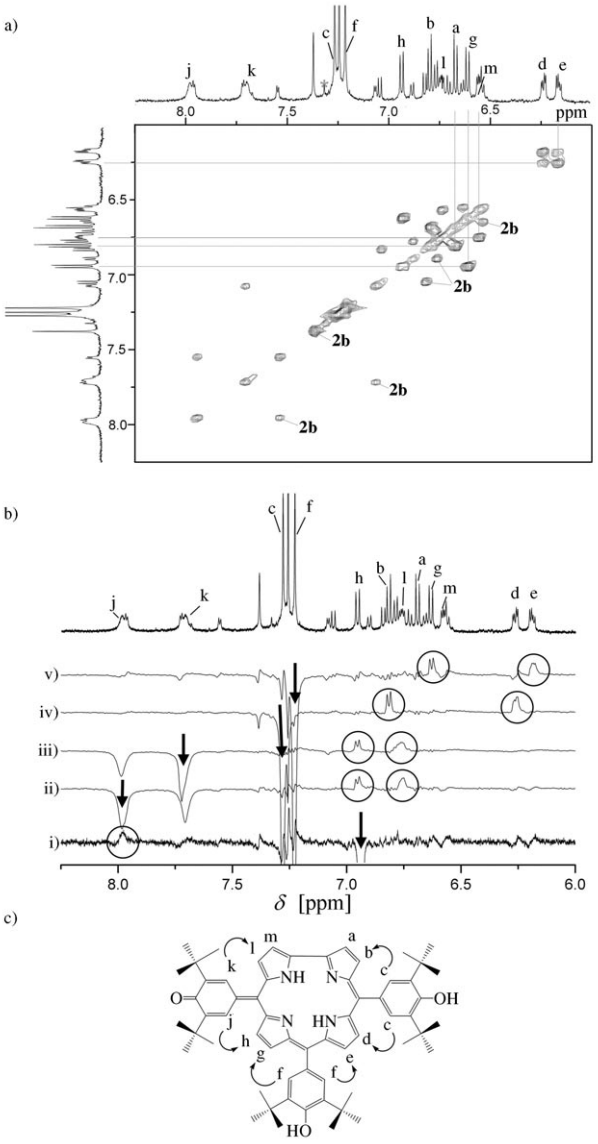

Figure 4. a) 2D-COSY (^{1}H,^{1}H) and b) i)–v) steady-state NOE enhancements obtained by irradiation at the indicated resonances of tautomer **2c** (downward arrows). Peaks and correlations due to **2b** are indicated. c) Assignments of peaks and elicited NOEs. Spectrum b) i) was used to differentiate between protons **j** and **k**.

these extremes are chemically identical. At room temperature, there should be an equilibrium between these two states leading to a broadening of the resonance due to the alkene proton of the quinone *meso*-substituent. One further indication of this non-coplanar arrangement is that there exists the possibility of an NOE enhancement of the signals of both pyrrole β-protons adjacent to this *meso*-substituent. The negative signal might then be due to mixing of the NOEs, although its intensity could suggest another mechanism. It should be noted that the quinone groups in the computed structure of **2b** are also non-coplanar, but the increased flexibility of the macrocycle compared to doubly intramolecularly hydrogen-bonded **2c** reduces the likelihood

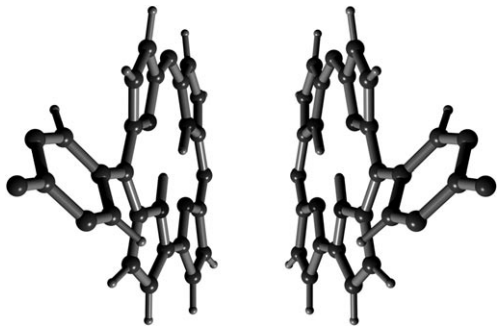

Figure 5. Model of the twisting about the lone quinonoid group in tautomer **2c**, which results in broadening of the resonance due to its alkenyl protons and permits an NOE with both pyrrole resonances adjacent to this substituent. Note that the conformers are chiral. *tert*-Butyl and other *meso*-substituents have been removed for clarity.

of observing a similar double NOE response. For **2c**, the positions of the NH protons could again be assigned based on the broadening of the corresponding β-pyrrole-H resonances.

To further observe the continuous change in the composition of the tautomeric mixture, a ^{1}H NMR titration of **2** in CD_2Cl_2 with [D_8]THF was conducted and the result is shown in Figure 6. As the proportion of [D_8]THF was increased, tautomers **2b** and **2c** gradually disappeared, which was accompanied by a concurrent increase in the proportion of **2a**. At the starting point of the titration (100 % CD_2Cl_2), **2c** accounted for around 80 mol % of the **2** present. The changes in the distribution of the tautomers during the titration are shown in Figure 6b. The existence of the discrete tautomers **2a**, **b**, and **c** can, in fact, be attributed to competitive intramolecular/intermolecular hydrogen bonding.[21]

The ^{1}H NMR spectra clearly demonstrate that both **2b** and **c** contain NH protons for which the chemical shifts ($13.5 < \delta < 18$ ppm) indicate the occurrence of hydrogen bonding, but these chemical shifts are not influenced by the presence of a hydrogen-bond acceptor, such as a polar solvent. For **2c**, this indicates two non-identical intramolecular hydrogen bonds, while **2b** possesses one imine group, which can be involved in an intramolecular hydrogen bond, leaving the two amine groups available for intermolecular hydrogen bonds. However, the titration indicates that for **2b** only one of these NH protons (that of ring c; see Figure 6a) actually interacts strongly with a hydrogen-bond acceptor (i.e. THF). This assignment can be made on the basis of the increased flexibility about ring c relative to that about ring a (see Figure 2a), and is consistent with the findings of an X-ray crystal structure determination for an *N*-alkyl derivative of **3** (see below).

In addition to the ^{1}H NMR spectroscopic studies, we performed a DFT computational analysis of the tautomers at the B3LYP/6-31G(d) level using the Gaussian program (see Figure 7). The energies of the tautomers relative to the porphyrinogen form **2a** proved to be consistent with the tautomeric assignment derived from the NMR data. Thus, tautomer **2b** is more stable than the other possible tautomers by

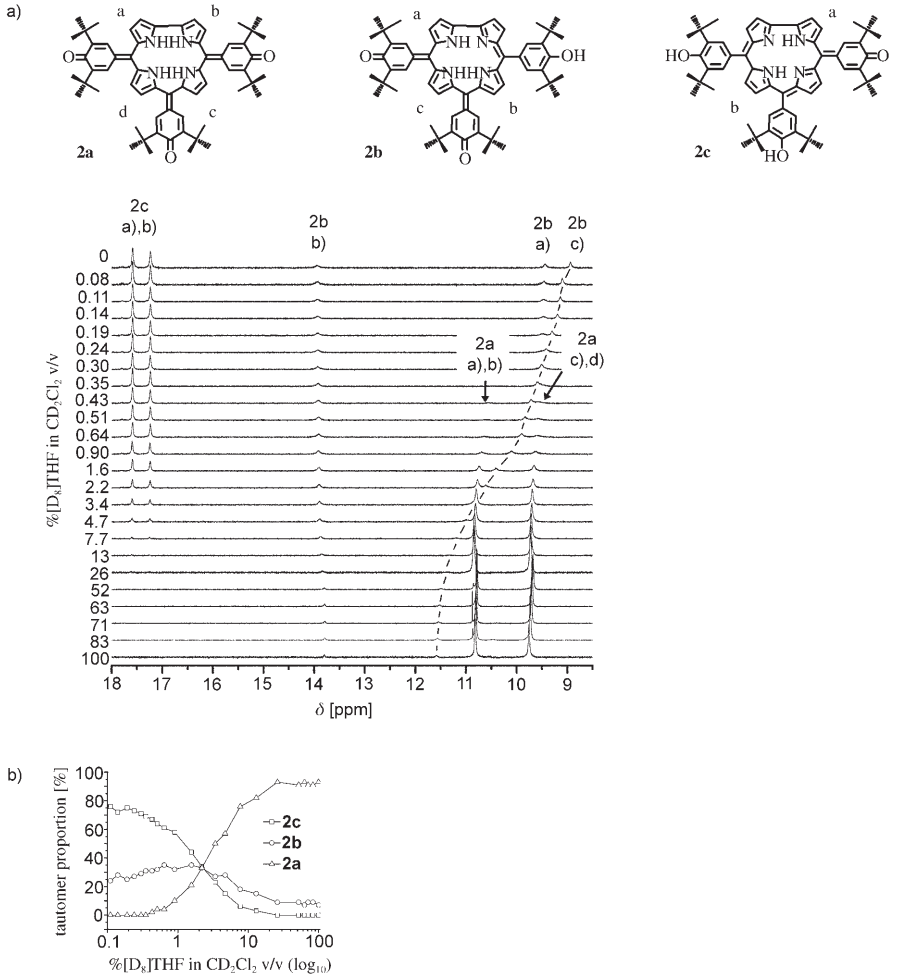

Figure 6. a) ^{1}H NMR titration of **2** in CD_2Cl_2 with [D_8]THF. b) Percentages of **2a**, **b**, and **c** during ^{1}H NMR titration of **2** in CD_2Cl_2 with [D_8]THF determined from the ratio of peak areas.

at least 7.43 kJ mol^{-1}. For **2c**, this value falls to 2.96 kJ mol^{-1}, although only two of the tautomers are stabilized, that is, one with the two phenol groups at the 5,10-positions and another with the phenol groups at the 5,15-positions. Taken together, the computed stability of the 5,10-tautomer relative to its 5,15-isomer and the presence of two phenol resonances in the ^{1}H NMR spectra support our assignment of the structure of **2c**. However, further computational analysis regarding the distribution of **2c** and its 5,15-isomer revealed an approximately 80:20 ratio of the two tautomers (see the Supporting Information), although this was difficult to confirm by ^{1}H NMR because of the proximity of the resonances of the phenolic protons. Additionally, the energy of the type 4 tautomer, bearing three phenol groups, relative to **2a** (+59.39 kJ mol^{-1}) was indicative of a substantial loss of stability, which helps to explain its absence from our observations of this system. The computed structures of the tautomers and their relative energies depend on the existence of intramolecular hydrogen-bonding interactions and how these influence the planarity of the tetrapyrrole. Thus, **2a** has all four central nitrogen atoms protonated, which precludes intramolecular H-bonds and imposes a porphyrinogen-like alternating puckered conformation of the pyrrole groups. **2b** has a single intramolecular H-bond, which reduces the flexibility of the macrocycle and induces some non-coplanarity of the quinone groups. The double intramolecular H-bonding in **2c** results in near-planarity of the macrocycle, forcing the remaining quinone group into a more non-coplanar conformation. The latter is reflected in the unusual NOE response for **2c** about the solitary quinone moiety. Notably, the possible tautomer **2c(i)** does not contain intramolecular H-bonds, perhaps because of steric effects, and this is reflected in its relatively poor stability.

In seeking a means of further controlling the tautomerism and to assist in the assignment of the relevant tautomer structures, *N*-alkylation of **2** was attempted using various alkylating agents. This resulted in complex mixtures of products, in contrast to the highly regioselective *N*-alkylation observed in the case of oxoporphyrinogen **1**.[24,25] However, one product, **3**, was obtained in unusually high yield and could be isolated in pure form following the alkylation of **2** using 4-nitrobenzyl bromide; its crystal structure is shown in Figure 8. Presumably, alkylation occurs preferentially at the porphyrin-type pyrrolic nitrogen because of the ease with which these groups achieve a porphyrinogen conformation relative to the α–α-linked corrole-type pyrrole groups. In the crystal structure of **3b**, exchangeable protons were located and their positions were refined, and bond length and bond angle analyses confirmed these locations. For the quinone oxygens O1 and O3, the C–O bond lengths are 1.2294(3) and 1.2400(3) Å, which correspond to C=O double bonds. The corresponding bond length for the phenolic C37-O2 bond is 1.3719(3) Å. The larger C–N–C bonding angles for N1, N2, and N4 relative to N3 indicate the NH character of these atoms. Furthermore, this crystal structure confirms the intramolecular hydrogen bonding between the proton at N2 and nitrogen N3. There is an intramolecular π–π stacking interaction between the phenyl group of the *N*-alkyl substituent and the *meso*-substituent at C5, with a centroid–centroid distance of 3.876(1) Å (see Figure 8). The molecular packing

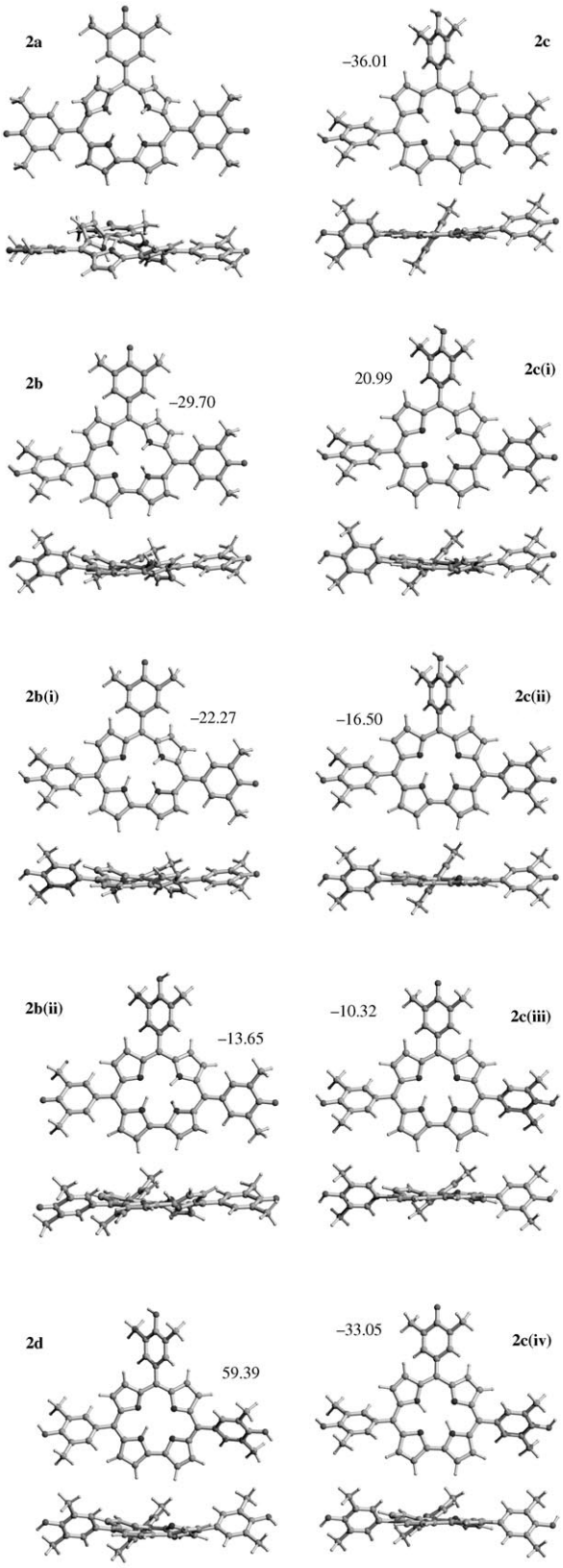

Figure 7. DFT computational analysis of the tautomers of **2** at the B3LYP/6-31G(d) level. Energy difference (ΔE in kJ mol^{-1}) of each possible tautomer is given relative to tautomer **2a**. Tautomers **2b** and **2c** are favored, supporting the assignment made on the basis of NMR spectroscopy.

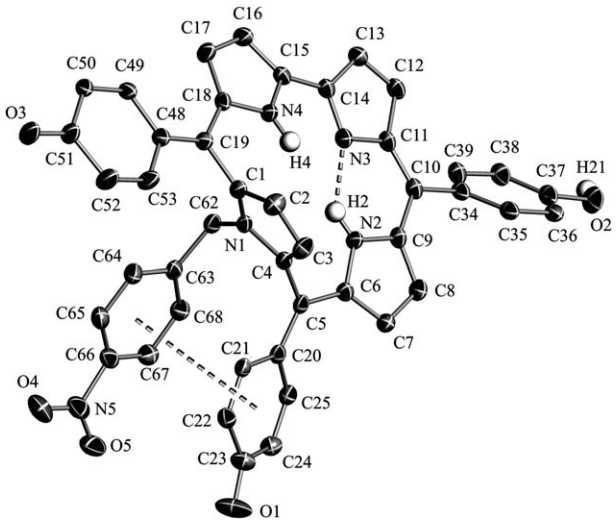

Figure 8. ORTEP representation of the X-ray structure of **3b** (*tert*-butyl groups and H-atoms bonded to C have been omitted for clarity) and its solvent-dependent tautomerism. Selected bond lengths and bond angles (Å or °): C23–O1 1.2294(3), C37–O2 1.3719(3), C51–O3 1.2400(3); C1-N1-C4 109.20(3), C6-N2-C9 111.21(3), C11-N3-C14 107.28(2), C15-N4-C18 112.66(3); N3···H2 1.9464(5); N3···H2-N2 132.16(3). Centroid (C20-C21-C22-C23-C24-C25)–centroid (C63-C64-C65-C66-C67-C68) distance: 3.876(1) Å.

is strongly influenced by intermolecular noncovalent interactions. First, a C–H···O interaction exists between the nitro group of the benzyl *N*-substituent and the methylene group of the corresponding substituent in a neighboring molecule (see Figure 9a). Second, the phenolic OH group is engaged in hydrogen bonding with a quinone oxygen atom of a 3,5-di-*tert*-butyl-4-oxocyclohexadienyl group, also in an adjacent molecule (see Figure 9b).

The most notable property of this molecule is that it still has the ability to tautomerize between forms **3a** and **b**

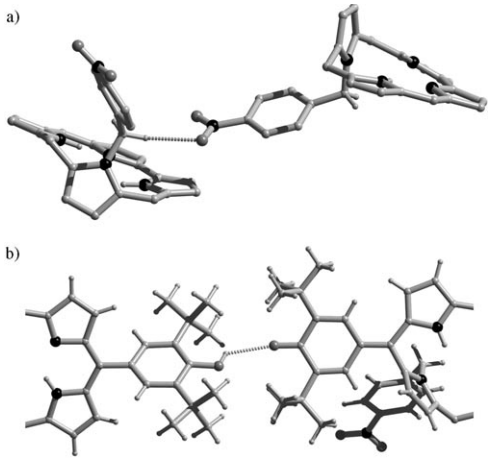

Figure 9. a) Intermolecular C–H···O hydrogen bond involving the nitro group in the X-ray crystal structure of **3b**. C–H···O bond length: 2.48 Å, angle: 153.99°. b) Hydrogen-bonding interaction between the phenolic O–H and a quinone group in an adjacent molecule of **3b**. O–H···O bond length: 2.39(2) Å, angle 128.9(17)°.

under control by solvent polarity, a feature that does not persist in the *N*-alkyl derivatives of **1**. Figure 10 shows the proton NMR spectra of the pure tautomers of **3**. The numbers of amine and phenol protons confirm the tautomeric assignments. In contrast to the mixture of **2b** and **c** in CD_2Cl_2, pure **3b** could be observed by NMR spectroscopy and its spectrum is consistent with the crystal structure. Furthermore, the crystal structure confirms intramolecular hydrogen bonding in **3a**, as was inferred for **2b** and **c** from their ^{1}H NMR spectra. The intramolecular hydrogen bonding is a key feature of this system since it confers both solvent dependency and thermal stability on the tautomers and permits us to control the tautomerism by varying the polarity of the medium under ambient conditions rather than by varying the temperature.

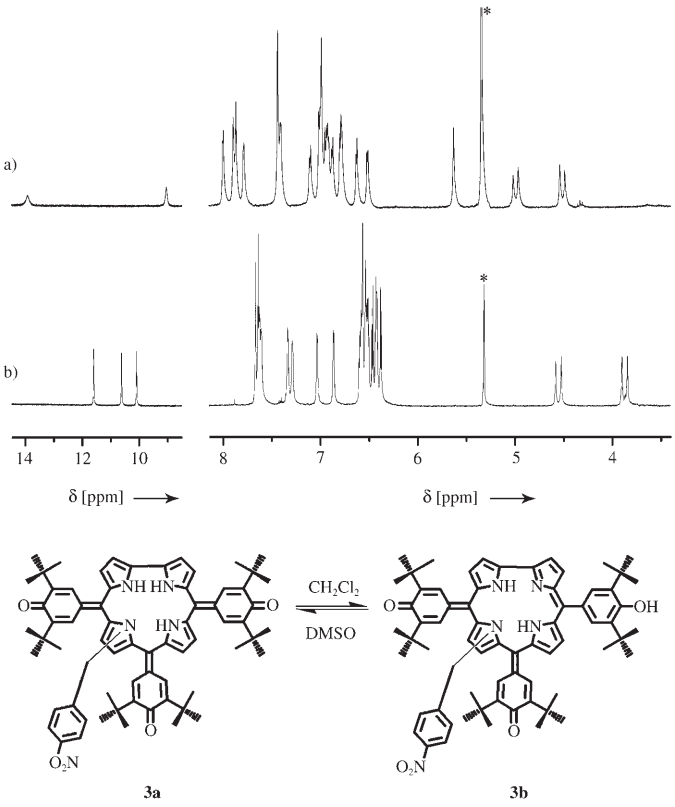

Figure 10. ^{1}H NMR spectra of **3** in a) CD_2Cl_2 (**3b**), b) $[D_6]$DMSO/CD_2Cl_2 (80% v/v) (**3a**) (*residual solvent).

The electronic absorption spectrum of the oxocorrologen **2** is dependent on both the nature of the solvent and the state of *N*-alkylation of the macrocycle. For solutions of **2** in dichloromethane, the absorption maximum appears at 450 nm and is accompanied by a broad absorption at 700 nm (see Figure 11). Interestingly, titration of a solution of **2** in dichloromethane with DMSO or methanol permits observation of the electronic spectrum of **2a**, in which all nitrogen atoms bear protons.

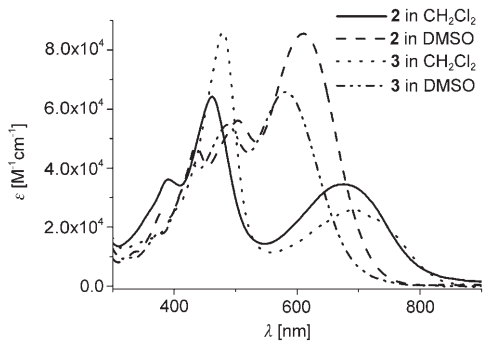

Figure 11. Electronic absorption spectra of **2** and **3** in the solvents indicated.

Further to the multiple tautomerism exhibited by **2** and its modulation by *N*-alkylation, the electrochemical behavior was investigated and compared with that of the structurally similar derivatives of **1**.[24c,d] Cyclic voltammograms of compounds **1**, **2**, and **3** in DMSO are shown in Figure 12. DMSO was chosen since in this solvent all of these compounds exist in the oxo (quinone) tautomeric form, that is, only one type of species was expected to be present. The redox processes were found to be irreversible, perhaps due to the associated electron/proton coupled reactions. Of interest are the values of the reduction potential and the HOMO–LUMO gap of **2** in comparison to those of **1**. Compounds **2** and **1** possess three and four hemi-quinonoid entities, respectively, and so reduction of **2** is expected to be more difficult than that of **1**. However, reductions of both **2** and **3** were found to be facile and were located at $E_{pc} = -1.17$ V vs Fc/Fc^+, as compared to a value of $E_{pc} = -1.32$ V vs Fc/Fc^+ for **1** in DMSO. This suggests increased electron deficiency of **2** as compared to **1**. An estimation of the HOMO–LUMO gap (the potential difference between the first oxidation and first reduction) also yielded a smaller value for **2** ($\approx$1.42 V) as compared to that for **1** (>1.53 V). In fact, oxidation of **1** could

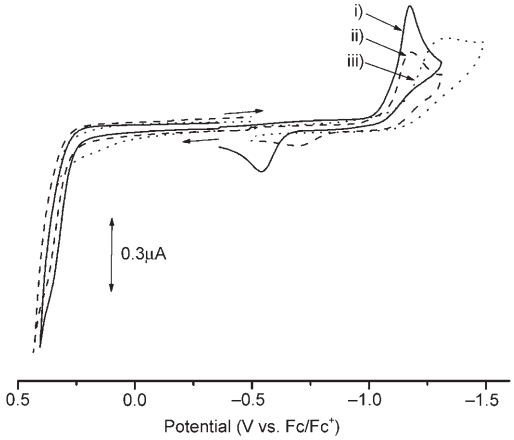

Figure 12. Cyclic voltammograms of i) **2**, ii) **3**, and iii) **1** in DMSO containing 0.1 M $(TBA)ClO_4$. Scan rate = 100 mV s^{-1}.

not be recorded within the anodic potential window of DMSO. The absorption spectra of **2** and **3** reveal red-shifted bands compared to the spectrum of **1** in DMSO, which may be attributed to the smaller HOMO–LUMO gap (see the Supporting Information). The facile reduction and smaller HOMO–LUMO gap for **2** as compared to **1** are noteworthy observations. The first reduction potentials of **2** and **3** are comparable to those of the widely used benzoquinone and fullerene electron acceptors,[26] suggesting that oxocorroles are promising candidates for use as components of novel donor–acceptor systems.

Conclusion

In summary, we have observed an unusual example of complex multiple tautomerism in a novel oxocorrole derivative. Alkylation of this compound at one macrocyclic nitrogen atom modulates the tautomerism and permits switching between two pure isomers of the *N*-alkyl oxocorrole by simple variation of solvent polarity. Isolation of the tautomers of **2** was more challenging, but high polarity yields a porphyrinogen form with other tautomers accessible at varying levels by changing the solvent polarity. Electrochemical studies have revealed electron deficiency and a smaller HOMO–LUMO gap for oxocorroles **2** and **3** as compared to oxoporphyrinogen **1**. We are currently seeking to control the tautomerism more finely by using a variety of stimuli. Furthermore, the construction of novel donor–acceptor systems through *N*-alkyl derivatization[24e] of oxocorroles to observe the effect of this tautomerization on potential intramolecular electron- and energy-transfer processes is currently underway. We believe that this system is an important initial step towards the development of a molecular switching manifold based on poly-tautomerism.

Experimental Section

General: Solvents and reagents used in this study were obtained from Aldrich Chemical Co., Tokyo Kasei Chemical Co., or Wako Chemical Co. Solvents for NMR spectroscopic measurements were obtained from Cambridge Isotope Laboratories Inc. Electronic absorption spectra were measured using a Shimadzu UV-3600 UV/Vis/NIR spectrophotometer. All ^{1}H NMR spectra were obtained using a JEOL AL300 BX spectrometer. Mass spectra were measured using a Shimadzu-Kratos Axima CFR+ MALDI-TOF mass spectrometer with dithranol as matrix. X-ray crystallography was carried out on a Bruker SMART Apex diffractometer equipped with a CCD area detector using $Mo_{K\alpha}$ radiation. Electrochemistry was performed using a three-electrode system. A platinum button electrode was used as the working electrode. A platinum wire served as the counter electrode and an Ag/AgCl electrode was used as the reference. Solutions were purged with argon prior to the electrochemical measurements. All experiments were carried out at 23 ± 1 °C.

Compound 2: Pyrrole (4.4 mL, 0.064 mol) was added to a refluxing mixture of propionic acid (300 mL) and 3,5-di-*tert*-butyl-4-hydroxybenzaldehyde (15 g, 0.064 mol) and reflux was continued for 3 h under air. The black solution was then concentrated to half of its original volume. The mixture was allowed to stand open to air at room temperature for 5 d, and then MeOH (200 mL) was added. The precipitate was collected by filtration, washed with MeOH, and chromatographed on silica gel eluting with dichloromethane. The second (dark-green) band eluting after the porphyrin by-product was collected and further purified by column chromatography (silica; CH_2Cl_2/hexane 2:3) to afford **2** as a dark-green microcrystalline solid (135 mg, 1%). ^{1}H NMR (CD_2Cl_2 containing 10% [D_6]DMSO, 300 MHz, 298 K): $\delta=11.75$ (br, 2H; NH), 10.94 (br, 2H; NH), 7.92 (s, 2H; cyclohexadienyl-H), 7.60 (s, 2H; cyclohexadienyl-H), 7.56 (s, 2H; cyclohexadienyl-H), 6.81 (d, ^3J(H,H) = 3.4 Hz, 2H; pyrrolic H), 6.71 (m, 4H; pyrrolic H), 6.63 (d, ^3J(H,H) = 3.4 Hz, 2H; pyrrolic H), 1.35, 1.29, 1.27 ppm (3×s, 54H; *t*Bu); UV/Vis (CH_2Cl_2): λ_{max} (ε) = 391 (36100), 462 (64200), 676 nm (34500 $mol^{-1}dm^{-3}cm^{-1}$); MALDI-MS (dithranol): *m*/*z*: 910 [M^+].

Compound 3: Compound **2** (18.2 mg, 0.02 mmol), 4-nitrobenzyl bromide (21.6 mg, 0.1 mmol), and K_2CO_3 (0.3 g, 2.2 mmol) were added to anhydrous ethanol (5 mL). The resulting mixture was refluxed under dry air for 7 h. The solvent was then removed under reduced pressure, the residue was dissolved in dichloromethane, and the resulting solution was washed with water and dried over Na_2SO_4. The crude product was purified by column chromatography on silica gel eluting with 50% dichloromethane in hexane to afford **3** as a dark-green solid (8.5 mg, 34%). ^{1}H NMR (CD_2Cl_2, 300 MHz, 298 K): $\delta=13.90$ (br, 1H; NH), 9.02 (br, 1H; NH), 7.97 (s, 1H), 7.86 (d, $^3J=8.5$ Hz, 2H), 7.76 (s, 1H), 7.38–7.41 (m, 3H), 7.08 (d, $^3J=4.1$ Hz, 1H), 6.96–6.99 (m, 3H), 6.89–6.93 (m, 2H), 6.85 (d, ^3J(H,H) = 4.4 Hz, 1H), 6.77 (d, ^3J(H,H) = 4.4 Hz, 2H), 6.60 (d, ^3J(H,H) = 3.7 Hz, 1H), 6.49 (d, ^3J(H,H) = 3.4 Hz, 1H), 5.60 (s, 1H; phenolic H), 4.97 (d, ^2J(H,H) = 15.4 Hz, 1H; benzylic H), 4.49 (d, ^2J(H,H) = 15.4 Hz, 1H; benzylic H), 1.07, 1.06, 1.02, 1.01, 0.93, 0.90 ppm (6×s, 54H; *t*Bu); UV/Vis (CH_2Cl_2): λ_{max} (ε) = 361 (16400), 479 (86400), 694 nm (26900 $mol^{-1}dm^{-3}cm^{-1}$); MALDI-MS (dithranol): *m*/*z*: 1044 [M^+].

X-ray crystallography: Crystals suitable for X-ray analysis were grown from a solution of **3** in dichloromethane/octane. **3b**·2 C_8H_{18}: $C_{84}H_{113}N_5O_5$, $F_W=1272.79$ $gmol^{-1}$, green block $0.42\times0.36\times0.29$ mm^3, monoclinic, $P2_1/c$, $a=20.7896(7)$, $b=14.6515(5)$, $c=25.7342(9)$ Å, $\beta=112.105(1)°$, $V=7262.4(4)$ Å^3, $F(000)=2768$, $\rho_{calcd}=1.146$ $gmol^{-1}$, $\mu(Mo_{K\alpha})=0.071$ mm^{-1}, $T=100$ K, 40778 data measured on a Bruker SMART Apex diffractometer, of which 13982 were unique ($R_{int}=0.0332$); 712 parameters refined against F_o^2 (all data), final $wR_2=0.1356$, $S=0.987$, R_1 (9803 data with $I>2\sigma(I)$) = 0.0503, largest final difference peak/hole = +0.62/−0.30 e Å^{-3}. Structure solution by direct methods and full-matrix least-squares refinement against F^2 (all data) using SHELXTL.[27] The coordinates of the NH and OH H-atoms were refined; H atoms bound to C were placed in calculated positions. The crystal structure contains two octane molecules of crystallization per corrole molecule; these were found to be severely disordered and were handled using the SQUEEZE option in PLATON.[28] CCDC 641061 (**3a**) contains the supplementary crystallographic data for this paper. These data can be obtained free of charge from The Cambridge Crystallographic Data Centre via www.ccdc.cam.ac.uk/data_request/cif.

Acknowledgements

This work was supported by a Grant-in-Aid for Science Research in a Priority Area "Super-Hierarchical Structures" from the MEXT, Japan, the National Science Foundation (Grant 0453464 to F.D.), the donors of the Petroleum Research Fund administered by the American Chemical Society, and the Deutsche Forschungsgemeinschaft.

[1] a) M. B. Smith, J. March, in *Advanced Organic Chemistry*, 5th ed., Wiley Interscience, New York, **2001**, pp. 1218–1223; b) J. Elguero, C. Marzin, A. R. Katritzky, P. Linda, in *The Tautomerism of Heterocycles, Adv. Heterocycl. Chem. Suppl. I*, Academic Press, New York, **1976**.

[2] a) H. Hart, *Chem. Rev.* **1979**, *79*, 515; b) Z. Rappoport, in *The Chemistry of Enols*, Wiley, Chichester, UK, **1990**.

[3] For example, the case of histamine: F. J. Ramírez, I. Tuñón, A. J. Collado, E. Silla, *J. Am. Chem. Soc.* **2003**, *125*, 2328–2340, and references therein.
[4] a) J. D. Watson, F. H. C. Crick, *Nature* **1953**, *171*, 737–738; b) J. D. Watson, F. H. C. Crick, *Nature* **1953**, *171*, 964–967; c) C. Colominas, F. J. Luque, M. Orozco, *J. Am. Chem. Soc.* **1996**, *118*, 6811–6821.
[5] a) P. Zuman, J. Michl, *Nature* **1961**, *192*, 655–657; b) M. Boiani, H. Cerecetto, M. González, O. E. Piro, E. E. Castellano, *J. Phys. Chem. A* **2004**, *108*, 11241–11248; c) P. Pérez, A. Toro-Labbé, *J. Phys. Chem. A* **2000**, *104*, 1557–1562.
[6] V. Balzani, M. Venturi, A. Credi, in *Molecular Devices and Machines*, Wiley-VCH, Weinheim, **2003**.
[7] P. Liljeroth, J. Repp, G. Meyer, *Science* **2007**, *317*, 1203–1206.
[8] a) P. Naumov, *J. Mol. Struct.* **2006**, *783*, 1–8; b) P. Naumov, A. Sekine, H. Uekusa, Y. Ohashi, *J. Am. Chem. Soc.* **2002**, *124*, 8540–8541; c) I. Renge, *J. Lumin.* **2000**, *98*, 213–220.
[9] J. R. Reimers, L. E. Hall, N. S. Hush, K. Silverbrook, *Ann. N. Y. Acad. Sci.* **1998**, *852*, 38–53.
[10] a) C. B. Storm, Y. Teklu, *J. Am. Chem. Soc.* **1972**, *94*, 1745–1747; b) J. Braun, M. Koecher, M. Schlabach, B. Wehrle, H.-H. Limbach, E. Vogel, *J. Am. Chem. Soc.* **1994**, *116*, 6593–6604.
[11] H. Furuta, T. Ishizuka, A. Osuka, H. Dejima, H. Nakagawa, Y. Ishikawa, *J. Am. Chem. Soc.* **2001**, *123*, 6207–6208.
[12] a) R. Paolesse, in *The Porphyrin Handbook, Vol. 2* (Eds.: K. M. Kadish, K. M. Smith, R. Guilard), Academic Press, San Diego, **2003**, pp. 201–232; b) R. Guilard, J.-M. Barbe, C. Stern, K. M. Kadish, in *The Porphyrin Handbook, Vol. 18* (Eds.: K. M. Kadish, K. M. Smith, R. Guilard), Academic Press, San Diego, **2003**, pp. 303.
[13] For example: a) G. Golubkov, Z. Gross, *J. Am. Chem. Soc.* **2005**, *127*, 3258–3259; b) J. P. Collman, M. Kaplun, R. A. Decreau, *Dalton Trans.* **2006**, 554–559; c) J.-M. Barbe, G. Canard, S. Brandes, F. Jérôme, G. Dubois, R. Guilard, *Dalton Trans.* **2004**, 1208–1214.
[14] I. Aviv, Z. Gross, *Chem. Commun.* **2007**, 1987–1999.
[15] a) Z. Gross, N. Galili, I. Saltsman, *Angew. Chem.* **1999**, *111*, 1530–1533; *Angew. Chem. Int. Ed.* **1999**, *38*, 1427–1429; b) R. Paolesse, L. Jaquinod, D. J. Nurco, S. Mini, F. Sagone, T. Boschi, K. M. Smith, *Chem. Commun.* **1999**, 1307–1308; c) D. T. Gryko, *Eur. J. Org. Chem.* **2002**, 1735–1743.
[16] Some rare examples of multiple protropic tautomerism: a) L. Szterenberg, L. Latos-Grażyñski, *J. Phys. Chem. A* **1999**, *103*, 3302–3309; b) K. Rachlewicz, N. Sprutta, P. J. Chmielewski, L. Latos-Grażyñski, *J. Chem. Soc. Perkin Trans. 2* **1998**, 969–975; c) H. Komber, H.-H. Limbach, F. Böhme, C. Kunert, *J. Am. Chem. Soc.* **2002**, *124*, 11955–11963.
[17] Corrole itself displays some propensity for tautomerism depending on its substituents: T. Ding, J. D. Harvey, C. J. Ziegler, *J. Porphyrins Phthalocyanines* **2004**, *9*, 22–27.
[18] a) L. R. Milgrom, *Tetrahedron* **1983**, *39*, 3895–3898; b) A. J. Golder, L. R. Milgrom, K. B. Nolan, D. C. Povey, *J. Chem. Soc. Chem. Commun.* **1989**, 1751–1753.
[19] a) L. R. Milgrom, J. P. Hill, W. D. Flitter, *J. Chem. Soc. Perkin Trans. 2* **1994**, 521–524; b) L. R. Milgrom, J. P. Hill, *J. Heterocycl. Chem.* **1993**, *30*, 1629–1633; c) L. R. Milgrom, J. P. Hill, W. D. Flitter, *J. Chem. Soc. Chem. Commun.* **1992**, 773.
[20] J. P. Hill, A. L. Schumacher, F. D′Souza, J. Labuta, C. Redshaw, M. J. R. Elsegood, M. Aoyagi, T. Nakanishi, K. Ariga, *Inorg. Chem.* **2006**, *45*, 8288–8296.
[21] M. S. Somma, C. J. Medforth, N. Y. Nelson, M. M. Olmstead, R. G. Khoury, K. M. Smith, *Chem. Commun.* **1999**, 1221–1222.
[22] Tautomeric switching between aromatic and anti-aromatic states of a 22-hydroxybenziporphyrin has recently been reported: M. Stêpieñ, L. Latos-Grażyñski, L. Szterenberg *J. Org. Chem.* **2007**, *72*, 2259–2270.
[23] S. Shimokawa, H. Fukui, J. Sohma, *Mol. Phys.* **1970**, *19*, 695–702.
[24] a) L. R. Milgrom, J. P. Hill, P. Dempsey, *Tetrahedron* **1994**, *50*, 13477–13484; b) L. R. Milgrom, J. P. Hill, G. Yahioglu, *J. Heterocycl. Chem.* **1995**, *32*, 97–101; c) J. P. Hill, I. J. Hewitt, C. E. Anson, A. K. Powell, A. L. McCarthy, P. Karr, M. Zandler, F. D′Souza, *J. Org. Chem.* **2004**, *69*, 5861–5869; d) J. P. Hill, W. Schmitt, A. L. McCarty, K. Ariga, F. D′Souza, *Eur. J. Org. Chem.* **2005**, 2893–2902; e) J. P. Hill, A. S. D. Sandanayaka, A. L. McCarty, P. A. Karr, M. E. Zandler, R. Charvet, K. Ariga, Y. Araki, O. Ito, F. D′Souza, *Eur. J. Org. Chem.* **2006**, 595–603.
[25] The related *N*-alkyl corroles are also known: Z. Gross, N. Galili, *Angew. Chem.* **1999**, *111*, 2536–2540; *Angew. Chem. Int. Ed.* **1999**, *38*, 2366–2369, and references therein.
[26] a) J. S. Connolly, J. R. Bolton, in *Photoinduced Electron Transfer, Part D* (Eds.: M. A. Fox, M. Chanon), Elsevier, Amsterdam, **1988**, pp. 303–393; b) M. E. El-Khouly, O. Ito, P. M. Smith, F. D′Souza, *J. Photochem. Photobiol. C* **2004**, *5*, 79–104.
[27] G. M. Sheldrick, SHELXTL 6.14, Bruker AXS Inc., 6300 Enterprise Lane, Madison, WI 53719-1173, USA (**2003**).
[28] A. L. Spek, PLATON—A Multipurpose Crystallographic Tool, Utrecht University, Utrecht (The Netherlands), **2002**; P. van der Sluis, A. L. Spek, *Acta Crystallogr.* **1990**, *A46*, 194.

Received: September 11, 2007
Published online: October 19, 2007

